J. King Saud Univ., Vol. 19, *Science* (1), pp. 59-71, Riyadh (1427H./2006)

Effect of Peak Shift on Planer and SPECT Images

S.H.A. Al-Lehyani
Physics Department, (Medical Physics Group), Faculty of Applied Sciences,
Um Al-Qura University, Makkah, Saudi Arabia
P .O. Box 10130
Tel:+966-2-5667624,
Email address: saud8882001@yahoo.com

(Received 30/4/1426H.; accepted for publication 29/11/1426H.)

Abstract. Gamma cameras are used to detect the radiopharmaceutical distributions in the patients organs. In the present work, investigation of the radiopharmaceutical distribution was carried out in one or more sections of some organs using the single photon emission computed tomography technique (SPECT) in which the gamma-camera detects the distribution of the injected radiopharmaceutical from varying angles around the patient's body at fixed intervals. To avoid interpretation mistakes, which can be generated due to protocol errors, the gamma camera must work at optimum conditions. One of these errors is the camera non-uniformity. This work aims to define the uniformity of the gamma camera which depends on many parameters such as the peak shift (off-peak) which is the shift of a specified radio isotope peak from its real position. In SPECT studies, the effect of the off-peak shift using heart phantoms, appears very important. Changes in the off-peak will affect the quality of the images very much leading to a different clinical diagnosis. It is concluded that the optimum off-peak is the 0% shift, but the data acquired in practice within the range of 0 to 2% off-peak shift does not affect the image quality considerably.

Keywords: Radionuclide imaging; SPECT; Physical factor.

Introduction

Nuclear medicine is a branch of medicine in which radioactive materials (unsealed source of radiation) are used for the diagnosis and treatment of different disorders. Diagnostic imaging of the lung, brain, thyroid, heart, liver,….., etc. is achieved using sophisticated gamma cameras, with topographic facilities linked to computer systems. Nuclear imaging technique is one of the most important tools for physicians to diagnose or to confirm a disease. The gamma camera is the most familiar imaging tool in nuclear medicine to obtain a good representative image, and too many steps must be carried out to obtain such an image. The patient is first injected by a suitable radioactive isotope which emits gamma rays that can be detected *in vivo* by a gamma camera. This would

give information on the physiology and radiopharmaceutical distribution in the organ of interest. The scintillation gamma camera is the most important detector. It consists of a detector head containing the collimator, the NaI(Tl) crystal and the photomultiplier tubes (PMTs). The head is mounted on a gantry that has the ability to move up and down or rotate through any angle. The console, houses the power supplies and the operational controls of the scintillation camera, including the display monitor. A computer is used for analyzing and displaying the recorded image [1].

A gamma ray image is projected by the collimator (thick slab of lead with a geometric array of holes) onto the NaI(TI) detector crystal, creating a pattern of scintillations in the crystal that outlines the distribution of radioactivity in front of the collimator. A photomultiplier (PM) tube array, viewing the back surface of the crystal, and electronic position logic circuits, determine the location of each scintillation event as it occurs in the crystal. Individual events are analyzed for energy by a pulse–height analyzer. When the event falls within the selected energy window, the electron beam in a cathode ray tube (CRT) is deflected by X- and Y-position signals to a location on the CRT face corresponding to the location at which the scintillation event occurred in the crystal. The beam is turned on causing a flash of light to appear at that point of the display, which can be recorded photographically.

In static imaging studies, the gamma camera is used to record the image of the static distribution of the radiopharmaceutical, and in dynamic imaging studies the camera is used for recording sequential images per suitable interval of time for the changes of the distribution of the radiopharmaceutical. Also, the camera can be used in single photon emission computed tomography (SPECT) imaging where several static images from different angles can be recorded, which are then reconstructed to give images of three dimensions [2]. The advantage of SPECT imaging is that out-of-plane information is removed and not simply blurred (but present) as in the earlier forms of tomography in nuclear medicine. Limited angle tomographic methods improved the image contrast to some degree and provided an enhanced view of sections of the patient, but were limited by crosstalk from out-of-plane slices, and inherently were not quantitative. Removing the out-of-plane information, SPECT significantly improves image contrast over planar imaging and has the ability to separate overlapping structures [3]. Camera system with two or more heads surrounding the patient with more detectors offer more optimal spatial resolution and sensitivity characteristics than are available with a single-head system. These combinations assume that the data from different heads are matched in gain, orientation and offset, so that the data can be combined. These systems also require more elaborate cards or automated devices to aid in changing the two or three collimators per system [4].

Quality control performed on nuclear medicine cameras provides the confidence to technologists and physicians that a SPECT scan supplies an accurate representation of the radioisotope distribution in the patient. Whereas planar detector quality control measures help to ensure high-quality planar imaging, SPECT imaging requirements place more stringent and additional performance requirements on a detector system. In

fact, it is possible that a camera which is functioning well as a planar instrument may produce artifacts in the SPECT image, which may adversely affect patient management. Guidelines for the frequency of QC testing and for the choice of tests to be performed at certain intervals [5] and are best reflected in the national electrical manufactures association (NEMA) standards.

Nuclear medicine imaging has not reached the level of standardization and automation because of the large number of parameters and other factors affecting image quality that each individual operator still has to choose or be aware before commencing imaging and emphasized on the crucial importance for ensuring the correct collection of the raw data. Errors in raw data can cause artifacts that are difficult or impossible to recognize and are the major causes of incorrect reporting [6-9]. Measurements of the effects of center-of-rotation (COR) shift of the rotating camera-based (SPECT) system on tomographic images have been defined [10]. Contrast and spatial resolution variations as a function of COR shift were measured for all shifts less than 1 pixel, in steps of 0.1 pixels. This region encompasses the typical COR variations. The behavior of these indices was analyzed. In addition, the validity of the limit imposed on the allowable COR shift, as utilized in the current SPECT quality control protocols, was examined [11]. The limits of either +/- 0.5 or +/- 0.25 pixels were used, these limits resulted in loss of resolution. The uncertainties in volume and concentration measurements were increased due to this resolution loss, for a COR shift of 0.25 pixels, the spatial resolution loss was approximately 5%. It was concluded that this small spatial resolution loss may not affect the qualitative evaluation of tomographic images. However, any loss of resolution should be avoided. For a COR shift of 0.1 pixels, the loss of resolution was not observed. This value should be a desirable choice as the maximum allowable COR shifts since it ensures the optimum performance of the SPECT system. SPECT using a rotating gamma camera needs accurate calibration of electromechanical components, detection system and reconstruction software [12]. A complete group of quality control procedures developed on the basis of experience and experimental data acquired using a series of widely used gamma camera SPECT systems was presented. The procedures have been divided into controls related to the rotational movement of the detector and controls on the principal physical parameters characterizing a tomographic image. The advances in gamma-camera design over the last 5 to 10 years have improved all aspects of image quality, particularly for tomographic imaging [12]. As system complexity increases, it becomes more important that both the technologist and physician be able to recognize the various types of artifacts that can occur in gamma-camera systems and their potential impact on clinical studies. The most sensitive indicator of gamma-camera performance is uniformity. Because this measurement is performed on a daily basis, it is the principle tool in evaluating the status of the gamma-camera. Most artifacts related to the integrity of the detector head, computer system, and hard copy device can be detected on the uniformity image. For tomographic imaging, a quantitative determination of uniformity is needed to ensure that the system will not introduce ring artifacts into the patient data. The action level for gamma camera non-uniformity is difficult because of the reproducibility of quality control measurements and service adjustments are usually unknown. The

reproducibility of integral uniformity (IU), differential uniformity (DU) and the corrected relative standard deviation (CRSD) had been evaluated [13] and the non-uniformity measured from the count stored in individual pixel values recorded can be calculated using the following formula:

For integral uniformity IU(%)=100 x (max-min)/(max+min)

For differential uniformity DU(%)=100 x (hi-low)/(hi+low)

where max and min are the maximum and minimum pixel counts and hi and low are the maximum and minimum %min pixel counts.

Material

A technetium generator model was used to produce a sterile solution of ^{99m}Tc as sodium pertechnetate. This solution is eluted using a 0.9% sterile and endotoxin free solution of sodium chloride from an alumina (AL_2O_3) chromatography column. The ^{99}Mo ($T_{1\backslash 2}$= 66.02h) parent of ^{99m}Tc ($T_{1\backslash 2}$= 6.02h) is adsorbed, where $^{99}Mo_{42} \rightarrow {}^{99m}Tc_{43}$ undergoes a β-decay in the generator. The daughter ^{99m}Tc is held chemically much less tightly than ^{99}Mo to the column material and the eluant, which consists of nearly pure Sodium Pertechnetate in, is then ready for combination with an agent to form the radiopharmaceutical.

The heart phantom consisted of a cardiac phantom inserted in an elliptical lung phantom which provides three dimensional source end density distributions that simulate cardiac imaging using ^{99m}Tc radio nuclides. Because of the elliptical design, the effects of non-uniform attenuation on SPECT imaging can be systematically studied along with non-uniform attenuation compensation techniques. In order to achieve a lung density between air and water, the lungs are filled with Styrofoam beads and are water tight for the addition of water. Since the human lung contains both water density material and air, this mixture of beads and water achieves a realistic overall lung density of roughly one-third that of water alone. The lung (an elliptical cylinder) and the cardiac insert can be filled independently. To prepare the lung heart phantom for imaging, the outer cavity of the heart phantom was filled with approximately 1.5 mCi of ^{99m}Tc and topped up to leave a small residual air bubble, then the heart phantom was inserted inside the lung phantom, and the lung phantom was filled with water through the filler holes in the top cover plate using a syringe.

The point source used was a small plastic cone containing a small ball of cotton with a ^{99m}Tc activity between 20-30μCi and this source represents the smallest concentrated source to avoid scatter, and thus to concentrate the radioactivity in a small and uniform size. The gamma camera used in this study was a dual head variable angle system, model E.Cam manufactured by Siemens.

Methods

The relation between the off peak in the integral differential center field of view (CFOV), and the useful field of view (UFOV) for different window widths was carried out. Changes in the off-peak were obtained by shifting the window by (2%, 3%, 4%, 5% and 6%) and using the following acquisition parameters:

matrix size 256 x 256, magnification 1.0, window width 10%, 15% and 20%, count rate 50K counts/s and collected count of 50,000,000 counts.

The off-peak shift was applied to obtain a thyroid scan and a renal scan after injecting the patient with 3 mCi ^{99m}Tc. Imaging was performed 20 minutes after injection and repeated four times using the same parameters each time. Effect of changing the off-peak shift to 0%, 2%, 4% and 6% were also performed using the following acquisition parameters: matrix size 256 x 256, magnification 3.2 for thyroid and 1 for renal window width of 15%, collected counts of 700,000 counts.

The effect of off-peak shift on SPECT images was also studied using the heart phantom. This study consisted of using the heart phantom in mult-SPECT acquisition for different off-peak shifts (2%, 4% and 6%) at five different windows width (5%, 10%, 15%, 20% and 25%) using the same parameters in each acquisition. The acquisition parameters were as follows:

matrix size 64 x64, magnification 1.45, window width (5%, 10%, 15%, 20% and 25%) count rate 50 K counts/s, rotation type (step and shoot), and orbit type (body contour), number of views per scan 32 and detectors configuration 90^{o}.

Results and Discussion

1. Effect of the off-peak on uniformity

1.1. at window width of 10%

The integral and differential uniformity values in both center field of view (CFOV) and useful field of view (UFOV) for 0, 2, 3, 4, 5 and 6% off-peak with 10% window width are presented in Table 1. Figures 1A and 1B show the integral and differential uniformity values in both CFOV and UFOV in arbitrary units versus the percentage off-peak in KeV with a window width of 10%. A small increase in the calculated values of the uniformity in the off-peak range from 0 to 3% can be easily noted in these figures indicating a small loss of uniformity. In the off-peak range from 3 to 5%, there is a decrease and a rapid increase in the integral values in both fields, CFOV and UFOV, whereas the differential values in both fields are suffering from rapid increase and decrease in uniformity, which indicates an instability in uniformity in that range.

Table 1. The calculated values of integral and differential uniformities in the center field of view (CFOV) and useful field of view (UFOV) for 0, 2, 3, 4, 5, and 6% off-peak at window width of 10%

Off peak%	Integral CFOV	Differential CFOV	Integral UFOV	Differential UFOV
0%	2.18	1.82	2.37	1.82
2%	2.22	1.75	2.82	2.09
3%	2.47	1.83	2.97	2.92
4%	2.93	2.09	3.31	2.35
5%	3.18	2.58	3.95	3.07
6%	4.61	3.17	4.99	3.35

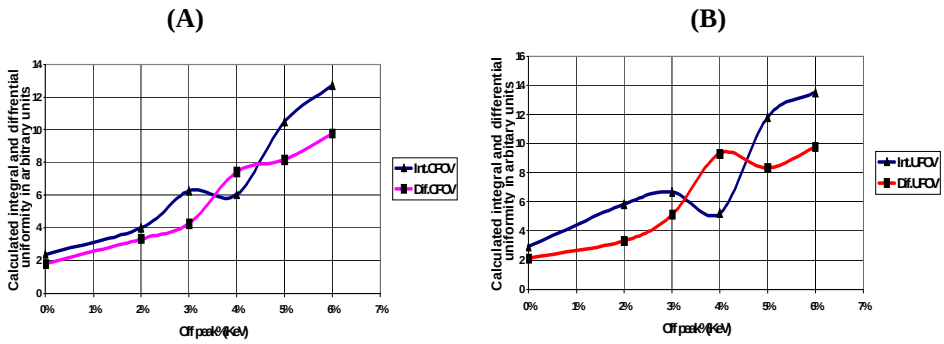

Fig. 1. The calculated integral (A) and differential uniformity (B) in CFOV & UFOV (arbitrary unites) versus off-peak percentage (KeV) at window width of 10%.

Figure 2 presents the images of flood for different uniformities due to the change in the off-peak percentage at a window width of 10%. Hot and cold areas (bright and dark spots) which are shown in the images (Fig. 2) offer an evidence of the decrease in uniformity with increasing the off-peak percentage. It can be also shown that the hot and cold areas can not be distinguished when visualized in the off-peak range from 0 to 3%, while in the off-peak range of more than 3% the quality of the image becomes worse.

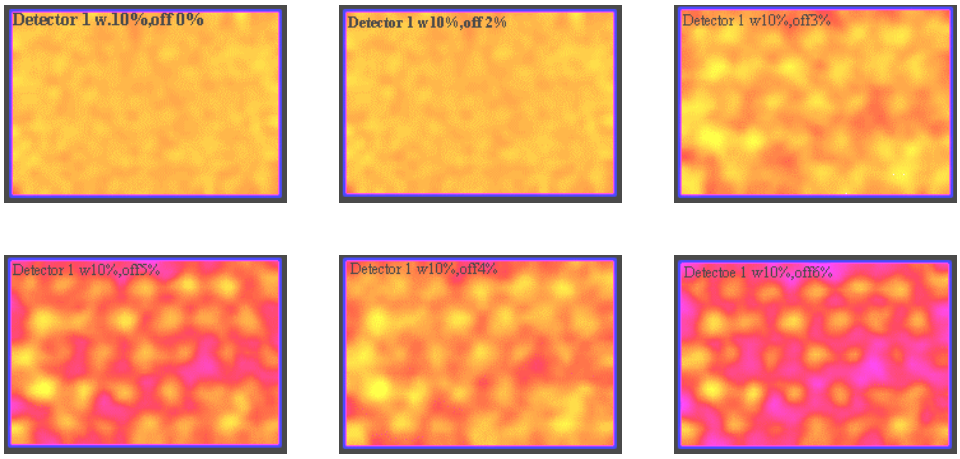

Fig. 2. Flood images for different off-peak percentage at window widthof 10%.

1.2. At window width of 15%

Figures 3A and 3B show the calculated integral and differential uniformity in both UFOV and CFOV versus the off-peak percentage at a window width of 15%. A small increase in the calculated values in both integral and differential uniformities can be noticed in the off-peak range from 0 to 2%, which indicates a little loss in uniformity. In the range from 2 to 3%, there is an increase in the calculated values giving more loss in both uniformities. In the rage from 3 to 4%, although the graph shows a flat curve (nearly stable uniformity values), however, it indicates more loss in the uniformity. There is a rapid increase in uniformity values in the off-peak range of more than 4%, which means that the uniformity becomes worse and worse.

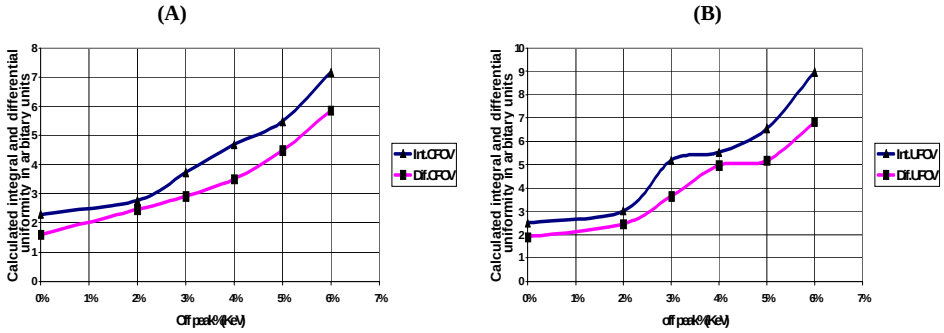

Fig. 3. The calculated integral (A) and differential uniformities (B) in CFOV & UFOV (arbitrary unites) versus of peak percentage (KeV) at window widthof 15%.

Figure 4 presents images of flood for different uniformities due to the change in the off-peak percentage at a window width of 15%. Hot and cold areas (bright and dark spots) which are shown in the images in Fig. 4 offer a good evidence on the decrease in uniformity

with the increasing of the off-peak percentage. It can be also shown that the differentiation between hot and cold areas is not clearly visualized in the off-peak range from 0 to 2%, while in the off-peak range of more than 2% the quality of the image becomes bad.

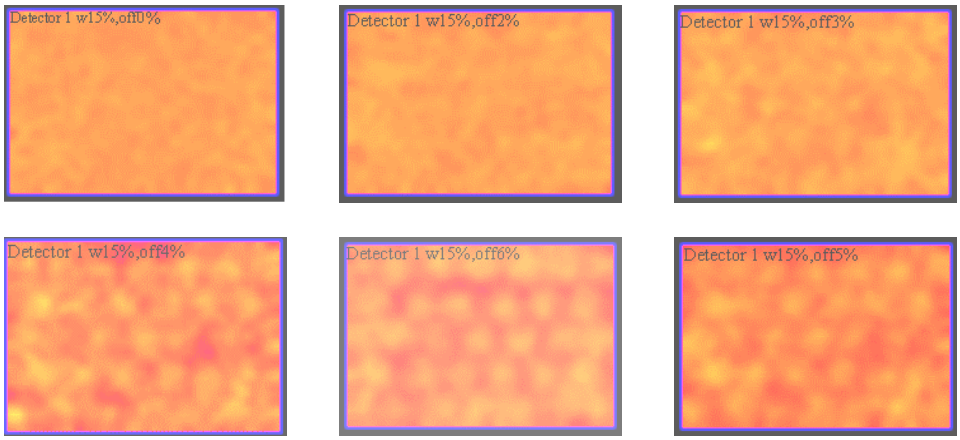

Fig. 4. Flood images for different off-peak percentage at window width of 15%.

1.3. At window width of 20%

Figures 5A and 5B show the calculated integral and differential uniformity in both UFOV and CFOV (arbitrary units) versus the off-peak percentage (KeV) at a window width 20%. When compared with Figs. 3A and 3B, no increase in the calculated values of both uniformities in the off-peak range from 0 to 3% as seen in Fig. 5A, which indicates good uniformity. On the other hand, Fig. 5B shows a small increase in the calculated uniformity values in the range from 2 to 3% which indicates bad uniformity in this range. Also, in the range from 3 to 4%, Fig. 5B shows a decrease in the calculated differential uniformity values (increase in the integral uniformity). At an off-peak shift of 4% and above there is a rapid increase in the calculated uniformity values which means that the uniformity becomes worse and worse.

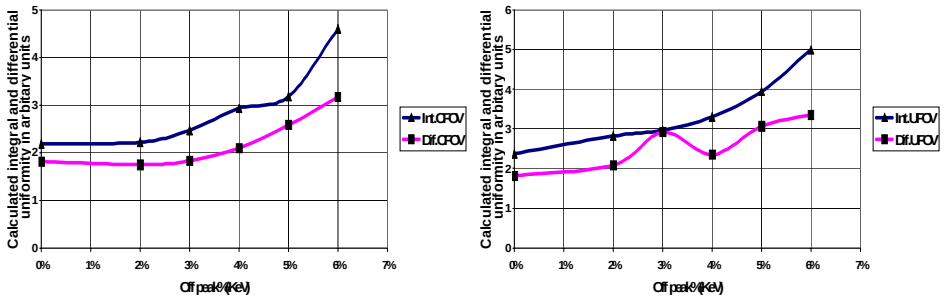

Fig. 5. Calculated integral (A) and differential uniformities (B) in CFOV & UFOV (arbitrary unites) versus off-peak percentage (KeV) at window widthof 20%.

Figure 6 presents flood images for different uniformities due to the change in the off-peak percentage at a window width of 20%. Hot and cold areas (bright and dark spots) which are shown in the images of Fig. 6 offer an evidence of the decrease in uniformity with increasing the off-peak percentage. It can be also shown that the differentiation between hot and cold areas is not clearly visualized in the off-peak range from 0 to 3%, while in the off-peak range of more than 3% the quality of the image becomes worse, so the change in the image is clearly visualized.

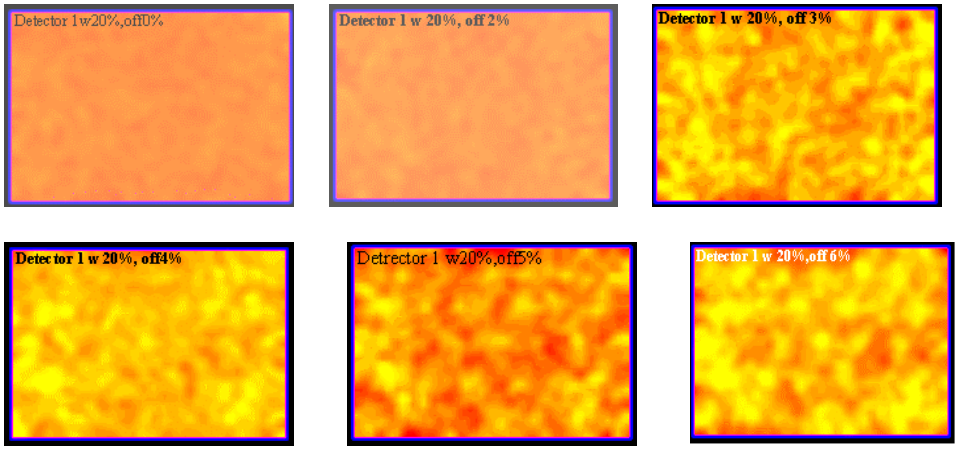

Fig. 6. Flood images for different off-peak percentage at window width of 20%.

2. Applied cases

2.1. Thyroid scan

Figure 7 shows four images of the thyroid taken for the same patient with different off-peak shifts 0%, 2%, 4% and 6%. These images show a decrease in the overall activity with a loss in the image quality.

The first image shows a normal and uniform tracer uptake pattern opposite both thyroid lobes with no focal lesions (i.e. normal morphology and function of the thyroid gland). In the second, third and forth images there is a decrease in the overall uptake in the salivary glands, thyroid gland and background, with no difference in sintigraphy diagnosis.

2.2. Renal scan

Figure 8 shows 4 images of a kidney scan taken for the same patient with different off-peak shifts of 0%, 2%, 4% and 6%. Different quality of images are shown in the scan, which indicates of change in the tracer distribution in the kidney.

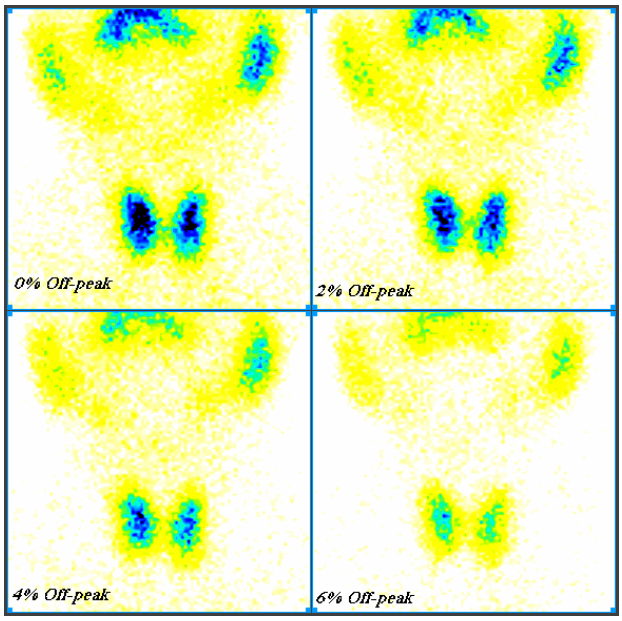

Fig. 7. Tc-99mThyroid scan: (1) 0% off-peak (2) 2% off-peak (3) 4% off-peak (4) 6% off-peak.

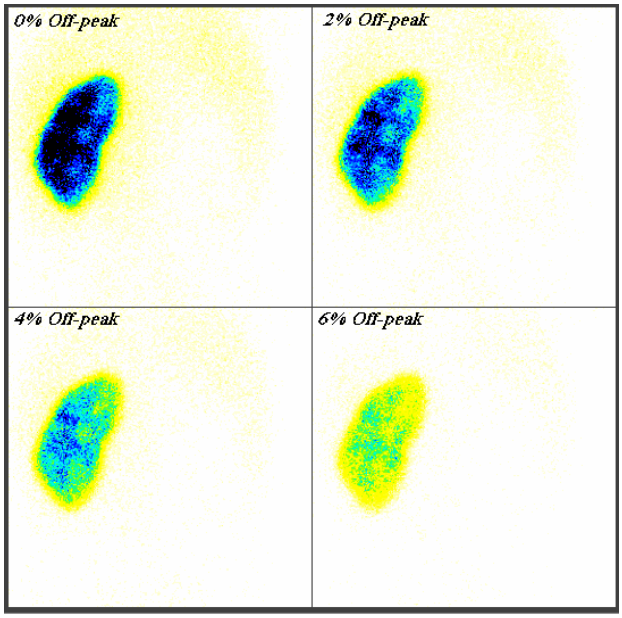

Fig. 8. Renal scan: (1) off-peak 0% (2) off-peak 2% (3) off-peak 4% (4) off-peak 6%.

The first image indicates normal (good and uniform tracer uptake pattern with normal cortical portrayal); the second image shows a mild decrease in overall tracer content which indicates of early diffuse parenchyma renal disease. The third image shows a moderate overall decrease in tracer uptake with moderately decrease in overall cortical tubular function. The fourth image shows marked decrease in renal uptake with thin (atrophic) cortex which can be attributed to chronic parenchyma renal disease with marked cortical tubular function loss. The off-peak percentage effect on SPECT images using heart phantoms shows four rows of vertical long axis cuts of the heart phantom SPECT study with 4 off-peak shifts at window width of 5% as shown in Fig. 9. The figure shows a loss in the recorded counts as seen in the rows from the upper one to the last one. This loss in the recorded counts may be due to the off-peak shift, which may result in an over estimating physician diagnostic.

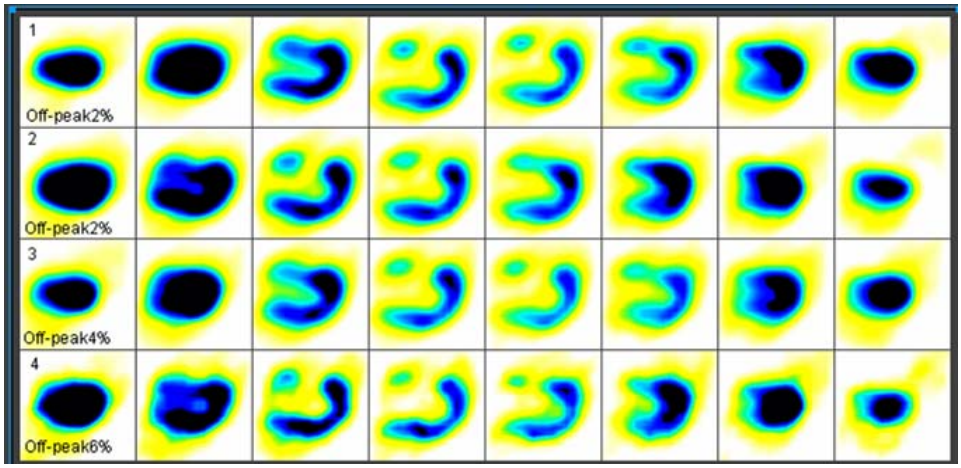

Fig. 9. Heart phantom SPECT study: (1) off-peak 0% (2) off-peak 2% (3) off-peak 4% (4) off-peak 6% at window width of 5%.

In the first to third rows, there is a single moderate sized perfusion defect that shows marked hypo-perfusion. Images in the forth row show degraded quality with exaggerated defect (large area of sever hypo-perfusion). In addition, the inferior wall shows a rather non-uniform tracer distribution. The fourth row image has a degraded quality with an exaggerated defect (large area of sever hypo-perfusion). In addition, the inferior wall shows rather non-uniform tracer distribution. Nearly the same views and results are repeated in the different off-peaks.

Conclusion

The effect of the off-peak shift on the uniformity at different window widths was performed and the effect of changes in the off-peak shift on calculated integral and differential uniformity was studied. A decrease in the differential uniformity and increase in the integral uniformity give an induction of the image quality.

The study of flood images obtained with different off-peak shifts showed differences in the images quality which could be due to the off-peak shift. It can be concluded that in planer and SEPECT images, the uniformity and quality of images are affected by a change of the off-peak shift and the effect becomes more pronounced at the peak shift of more than 2%. Thus, it is recommended that gamma camera used for this purpose should be operated with off-peak shifts less than 2% otherwise images with bad quality and uniformity will lead to foul diagnosis.

References

[1] Early, P. J. *Textbook of Nuclear Medicine Technology*. 4th ed., Mosby 1995.

[2] Sorenson, J.A. and Phelps, M.E. *Physics in Nuclear Medicine*. 2nd ed., Grune & Stratton, Inc., 1987.

[3] Groch, M.W. and Erwin, W.D. "SPECT in Year 2000: Basic Principles." *J. N. M. Technology,* 28, No. 4 (2000), 233-244.

[4] Spies, S.M. "Oral Communications: An Example of an Initial Bone Scan Using the Starbrite TM Crystal System." Sept. 2000.

[5] NEMA. *Performance Measurements of Scintillation Cameras, Standards Publication No. 1*. NEMA, 1994.

[6] Groch, M.W. and Erwin, W.D. "Single-photon Emission Computed Tomography in the Year 2001." *Instrumentation and Quality Control, J. N. M. Technology,* 29 (2001), 12-18.

[7] DePuey, E.G. "How to Detect and Avoid Myocardial Perfusion SPECT Artifacts." *J.N.M.*, 35, No. 4 (1994), 699-702.

[8] Graham, L.S. "Quality Control for SPECT Systems Radiography." 15, No. 6 (1995), 1471-1481.

[9] Baron, J.M. and Chouraqui, P. "Myocardial Single-photon Emission Computed Tomography, Quality Assurance." *J. Nucl. Cordial,* 3, No. 2 (1996), 157-166 .

[10] Saw, C.B. "Effects of Center-of-rotation Shift on Contrast and Spatial Resolution of the SPECT System". *Nucl. Med. Commun.,* 7, No. 5 (1986), 373-379.

[11] Agostini, A.; De Zatta, G.; Bagliani, G. and Tarolo, G.L. "Proposal for a Quality Control Procedure for Rotating Gamma Camera Tomographic Systems." *Radiol Med (Torino),* 74, No. 1 & 2 (1987), 109-115.

[12] O'Connor, M.K. "Instrument and Computer Related Problems and Artifacts in Nuclear Medicine." *Semin. Nucl. Med*., 26, No. 4 (1996), 256-277.

[13] Young, K.C.; Kourisk, A.M. and Abdel-Dayem, H.M. "Reproducibility and Action Levels for Gamma Camera Uniformity." *Nucl. Med. Commun.*, 11, No. 2 (1990), 95-101.

مدى تأثير الإزاحة العظمى للصورة باستخدام الفوتون أحادي الانبعاث

سعود بن حميد اللحياني

قسم الفيزياء، (مجموعة الفيزياء الطبية)،

كلية العلوم التطبيقية، جامعة أم القرى،

مكة المكرمة، المملكة العربية السعودية،

ص ب ١٠١٣٠، هاتف: ٠٠٩٦٦٢٥٦٦٧٦٢٤

البريد الإلكتروني: saud8882001@yahoo.com

(قدم للنشر في ١٤٢٦/٤/٣٠هـ؛ وقبل للنشر في ١٤٢٦/١١/٢٩هـ)

ملخص البحث. تستخدم كاميرات أشعة جاما في الكشف عن توزيعات العقاقير المشعة في أعضاء جسم الإنسان. وفي هذا البحث تمت دراسة هذا التوزيع للعقار المشع داخل قطاع أو أكثر لبعض أعضاء الجسم باستخدام تقنية الفوتون أحادي الانبعاث حيث يتم حقن العقار المشع ثم تدور الكاميرا حول جسم المريض من زاويا مختلفة لفترات زمنية ثابتة لتصوير العقار المشع. ولكي نتجنب حدوث أخطاء في البرتوكول المستخدم لا بد لكاميرا أشعة جاما أن تكون في أفضل الظروف والحالات. إن أحد هذه الأخطاء هي عدم انتظامية الكاميرا المستخدمة. ولهذا فإن البحث الحالي يهدف لتعريف هذه الانتظامية والتي تعتمد بدورها على عوامل كثيرة. وأهم هذه العوامل هي الإزاحة العظمى لقراءة المادة المشعة عن موقعها الأصلي. إن مثل هذه الإزاحة ذات أهمية خاصة عند استخدام بدائل مماثلة للقلب لدراسة توزيع العقار المشع فيها إذ أنها تؤثر على جودة الصورة الناتجة مما يؤدي بدوره إلى أخطاء في التشخيص الإكلينيكي. وقد توصل هذا البحث إلى أن أحسن جودة للصورة هي تلك التي تكون فيها إزاحة القراءة العظمى تساوي صفر، إلا أن الواقع العملي أثبت أن مثل هذه الجودة للصورة يمكن الحصول عليها في المدى ما بين صفر إلى ٢٪.